Biochimica et Biophysica Acta 1788 (2009) 1064–1072

Contents lists available at ScienceDirect

Biochimica et Biophysica Acta

journal homepage: www.elsevier.com/locate/bbamem

Activation of phospholipase A_2 by temporin B: Formation of antimicrobial peptide-enzyme amyloid-type cofibrils

Christian Code [a], Yegor A. Domanov [a], J. Antoinette Killian [b], Paavo K.J. Kinnunen [a,*]

[a] Helsinki Biophysics and Biomembrane Group, Medical Biochemistry, Institute of Biomedicine, P.O. Box 63 (Haartmaninkatu 8), FIN-00014, University of Helsinki, Finland
[b] Chemical Biology and Organic Chemistry Research Group, Bijvoet Center for Biomolecular Research/Institute of Biomembranes, Department of Chemistry, Faculty of Science, Utrecht University, The Netherlands

ARTICLE INFO

Article history:
Received 15 September 2008
Received in revised form 3 March 2009
Accepted 3 March 2009
Available online 11 March 2009

Keywords:
Phospholipase A2
Temporin
Antimicrobial peptide
Lag-burst kinetics
Interfacial activation
Fluorescence
Resonance energy transfer
FRET
Oligomerization
Amyloid fibril
Copolymerization

ABSTRACT

Phospholipases A2 have been shown to be activated in a concentration dependent manner by a number of antimicrobial peptides, including melittin, magainin 2, indolicidin, and temporins B and L. Here we used fluorescently labelled bee venom PLA2 (PLA2D) and the saturated phospholipid substrate 1,2-dipalmitoyl-glycero-*sn*-3-phosphocholine (L-DPPC), exhibiting a lag-burst behaviour upon the initiation of the hydrolytic reaction by PLA2. Increasing concentrations of Cys-temporin B and its fluorescent Texas red derivative (TRC-temB) caused progressive shortening of the lag period. TRC-temB/PLA2D interaction was observed by Förster resonance energy transfer (FRET), with maximum efficiency coinciding with the burst in hydrolysis. Subsequently, supramolecular structures became visible by microscopy, revealing amyloid-like fibrils composed of both the activating peptide and PLA2. Reaction products, palmitic acid and 1-palmitoyl-2-lyso-glycero-sn-3-phosphocholine (lysoPC, both at >8 mol%) were required for FRET when using the non-hydrolysable substrate enantiomer 2,3-dipalmitoyl-glycero-*sn*-1-phosphocholine (D-DPPC). A novel mechanism of PLA2 activation by co-fibril formation and associated conformational changes is suggested.

1. Introduction

Phospholipases A2 (PLA2) constitute a group of ubiquitous enzymes serving a plethora of functions, from toxicity of insect and snake venoms to phospholipid metabolism, digestion, cellular signaling, and antimicrobial activity [1]. These enzymes hydrolyze the *sn*-2 acyl chain from glycerophospholipids to yield free fatty acids (FFA) and lysophospholipids, and both their catalytic mechanism as well as structures are conserved, with a high degree of sequence homology between different species, in particular for secretory PLA2s [1,2].

Similarly to the other lipolytic enzymes, PLA2 exhibits the so-called interfacial activation: compared to the hydrolysis of monomeric lipids their activity is dramatically enhanced when reacting with substrate interfaces [3], such as present in micelles, monolayers, and bilayers. *The enzyme model* assumes a change in the PLA2 conformation to be caused by the interface [4], while *the substrate model* assigns the activation to the altered physicochemical properties of the substrate when present in the interface [5]. Accordingly, the activity of PLA2 is influenced by the lipid composition and the phase state of the substrate phospholipids [6], negatively charged phospholipids [7], lipid lateral packing density [8], lipid protrusions [9], and membrane curvature [10,11]. Additionally, the influence of an electric field [12] and effects by membrane associating small molecules have been reported (for a brief recent account see Code et al. [13]). Changes in PLA2 conformation upon interfacial activation have been demonstrated and it was suggested that enzyme conformational alterations, in unison with the physical state of the substrate, would cause the augmented catalytic activity [14,15]. Notably, Hille et al. as well as Dennis and co-workers concluded the activation of PLA2 to be accompanied by its aggregation at interfaces [16,17], as visualized in 1,2-dipalmitoyl-*sn*-glycero-3-phosphocholine (L-DPPC) monolayers [18-20]. More detailed characteristics of the aggregated PLA2 were recently described by us [13], providing evidence for the activation of

Abbreviations: apoC-II, apolipoprotein C-II; CD, circular dichroism; C-temB, cysteine-temporin B; L-DPPC, 1,2-dipalmitoyl-*sn*-glycero-3-phosphocholine; D-DPPC, 2,3-dipalmitoyl-*sn*-glycero-1-phosphocholine; DHPC, 1,2-dihexadecyl-*sn*-glycero-3-phosphocholine; DIC, differential interference contrast; FFA, free fatty acid; FRET, Förster resonance energy transfer; γ, lag time; LPL, lipoprotein lipase; LUV, large unilamellar vesicles; lysoPC, 1-palmitoyl-2-hydroxy-*sn*-glycero-3-phosphocholine; PA, palmitic acid; PAGE, sodium dodecyl sulfate polyacrylamide gel electrophoresis; PLA2, phospholipase A_2; PLA2D, phospholipase A_2 labeled with Alexa 488 (donor); *r*, anisotropy; SDS, sodium dodecyl sulfate; *sn*, stereochemical notation; τ, fluorescence lifetime; temB, temporin B; T_m, main phase transition temperature; ThT, Thioflavin T; TRC-temB, cysteine-temporin B labelled with Texas Red

* Corresponding author. Fax: +358 9 19125444.
E-mail address: paavo.kinnunen@helsinki.fi (P.K.J. Kinnunen).

0005-2736/$ – see front matter © 2009 Elsevier B.V. All rights reserved.
doi:10.1016/j.bbamem.2009.03.002

PLA2 at a substrate interface to involve the formation of amyloid-type oligomers. Formation of fibrillar structures upon the action of PLA2 on supported phosphatidylcholine bilayers was recently observed by AFM [21].

Several amyloidogenic peptides, e.g. amyloid Aβ-peptides [8], and several antimicrobial peptides (AMPs), e.g. temporin B (temB) and temporin L, indolicidin, magainin 2 [22], LL-37 [23], bombolitin III [24], and melittin [25,26], enhance the activity of PLA2. Characteristically these peptides are cationic and amphiphilic, promote the segregation of negatively charged phospholipids, and partition into membranes [27,28]. In order to pursue the mechanism of the activation of PLA2 by AMPs in more detail we used C-temB (CLLPIVGNLLKSLL-$CONH_2$), i.e. temB with an additional N-terminal cysteine. The latter allows an easy covalent labelling with fluorophore maleimide and we have shown a Texas Red derivative of this peptide (TRC-temB) to have essentially similar antimicrobial and lipid binding properties as the natural temB [29]. TemB belongs to temporins, a family of AMPs now comprising of 76 different peptides, isolated from the skin of the European red frog, *Rana temporaria* [30]. The amphipathicity and net positive charge of temB allows it to penetrate into membranes and concentrate on negatively charged membranes, segregating with anionic lipids [28]. TemB thus efficiently perturbs lipid bilayers and causes membrane permeabilization [28,31,32]. Analogously to most AMPs characterized so far, the membrane intercalation of temB is prevented by cholesterol [28,29]. Similarly to LL-37, plantaricin A, and another member of the temporin family, temporin L, temB as well as TRC-temB have been shown in model membranes to aggregate and form amyloid-like Congo-red staining fibers, driven by both electrostatics and hydrophobicity [29,33,34].

Here we report the activation of bee venom PLA2D by TRC-temB to be accompanied by a shortening of the lag time and an augmented burst in the hydrolysis of a saturated phospholipid substrate, DPPC. We demonstrate close interactions between the peptide and the enzyme, as observed by Förster resonance energy transfer (FRET). At the end of the reaction, sub-millimetre amyloid-like fibrils composed of both PLA2D and TRC-temB were present. TemB is suggested to promote the nucleation of the growth of amyloid-like fibrils by PLA2, resulting in the formation of peptide-enzyme cofibrils, which causes a conformational change in the enzyme, yielding an augmented expression of its catalytic activity.

2. Materials and methods

2.1. Materials

L-DPPC was from Avanti Polar Lipids (Alabaster, AL), and D-DPPC and 1,2-dihexadecyl-*sn*-glycero-3-phosphocholine (DHPC) from Sigma-Aldrich. Thin layer chromatography of these lipids was performed on silicic acid coated plates (Merck, Darmstadt, Germany) developed with a chloroform/methanol/water mixture (65:25:4, v/v/v). Examination of the plates after iodine staining revealed no impurities. Bee venom PLA2 was from Sigma and its purity was verified by polyacrylamide gel electrophoresis in the presence of sodium dodecyl sulphate (PAGE). Fluorescent labels Alexa Fluor 488 carboxylic acid, succinimidyl ester, and Texas Red C_2 maleimide were from Invitrogen/Molecular Probes (Eugene, OR). All other chemicals were of analytical grade and from standard sources. Concentrations of the lipid stock solutions in chloroform were determined gravimetrically with a high-precision electrobalance (Cahn, Cerritos, CA), as described in detail by [35,36]. Freshly deionized filtered water (Milli RO/Milli Q, Millipore Inc., Jeffrey, NH) was used in all experiments. Protein, lipid, and $CaCl_2$ solutions were prepared and passed through a 0.2 μm filter (Schleicher and Shuell Microscience, Dassel, Germany) prior to use. C-temB (CLLPIVGNLLKSLL-CONH2) was from Synpep (Dublin, CA) and its purity was checked by HPLC (purity>95%) and sequence confirmed by mass spectrometry [29].

2.2. Preparation of labelled phospholipase A_2 and temporin B

Covalent coupling of the Alexa 488 fluorophore to PLA2 was conducted following the instructions of the manufacturer of the dye. The concentration of PLA2 was calculated from UV spectra using $E^{1\%}_{280} = 13.0$ and MW = 15,249 [37]. The concentration of the carboxylic acid succinimidyl ester of the Alexa 488 dye (MW = 643.4) was determined using a molar extinction coefficient of 71,000 $M^{-1}cm^{-1}$ at 495 nm. Absorption spectra were measured with a spectrophotometer (Perkin Elmer Lambda Bio40 UV/Vis, Boston, MA) using 10 mm path length quartz cuvettes (Hellma, Essex, UK) and 2 nm bandpass. For labelling 0.2 mM PLA2 and 0.3 mM dye were reacted for 1 h at 25 °C with magnetic stirring and protected from light in a total volume of 100 μl of 100 mM Na_2HCO_3, pH 8.3. At this pH the dye couples primarily to aliphatic amines. Chromatography on prepacked columns (Biospin 6, Hercules, CA) with an exclusion limit of 6000 Da was used to change the buffer to 5 mM HEPES, 0.1 mM EDTA, pH 7.5, and to remove any unreacted dye. The extent of labelling (dye to protein molar ratio) was determined by UV spectroscopy. Correction factor for the extinction coefficient in the determination of the dye content of the labelled enzyme at 280 nm was 0.11. The final dye/protein molar ratio varied from 0.6:1 to 1:1, as indicated. The labelled enzyme was stored in 20 μl aliquots at −20 °C prior to use. The bee venom PLA2 was chosen for the current study as it has been shown to bind to lipid membranes by non-electrostatic interactions with no preference for negatively charged phospholipids over zwitterionic ones [37]. Therefore, even though the fluorescent label used by us is expected to react with Lys residues this should have an insignificant effect on the primary enzyme-substrate interaction between the labelled PLA2 and DPPC.

Labelling of Cys-temporin B (C-temB) was performed as described by Sood et al.[29]. In brief, a 1:1 molar ratio mixture of C-temB and Texas Red maleimide at final concentrations of 50 μM in 20% acetonitrile, 20 mM Hepes, 0.1 mM EDTA, pH 7.0 was incubated for 3 h at room temperature in the dark with magnetic stirring. Labelled peptide was purified by reversed phase HPLC (μRPC C2/C18/ ST 4.6/100 column, ÄKTA Purifier, Amersham) eluting with a gradient of 10 to 80% acetonitrile with 0.05% trifluoroacetic acid. No unreacted Texas Red maleimide was detected indicating that the peptide was completely labelled. This was further confirmed by mass spectrometry using Flex Control MALDI-TOF spectrometer (Bruker Daltonics, Bremen, Germany) and a saturated solution of α-cyano-4-hydroxycinnamic acid as a matrix. The concentration of the Texas Red labelled peptide was determined using molar extinction coefficient of 112,000 $M^{-1}cm^{-1}$ at 589 nm. No major influence by the fluorophore on the lipid binding properties of temB was observed [29]. Apparently, the hydrophobicity of the latter exceeds as such, without the contribution of the hydrophobicity of the fluorophore, what is needed for the proper lipid binding of this peptide.

2.3. Assessment of the lag-burst behaviour in the PLA2 reaction

Similarly to other PLA2s the bee venom enzyme shows a distinct lag time γ in its hydrolytic action on DPPC liposomes [13], defined as the latency period between the addition of the enzyme and the burst in the catalytic rate. The lag was determined by measuring the decrease in pH with a miniature electrode (Microelectrodes, Bedford, New Hampshire, USA) inserted into the fluorescence cuvette (see below). Importantly, as we only wanted to observe the lag period and define the time point of the subsequent burst we did not correct for the decrement in pH by titration with a base. Accordingly, only semiquantitative data on the PLA2 activity are obtained. The burst was determined as the intersection point of the linear fits to the pH curve during the lag and the initial phase of rapid hydrolysis. For saturated

phospholipid substrates such as DPPC the length of the lag time varies considerably with temperature, having minimum at the main phase transition T_m [6,38]. In order to have a clearly discernible lag the experiments described herein were performed at 37 °C. Under the conditions employed (viz. 200 μM DPPC, 75 nM PLA2D, T = 37 °C) a latency period of about 30 min preceded the burst in activity evident as a decrease in pH (Fig. 1A; Fig. 2). In our previous study [13] we observed no major difference in the lag for the labelled and native PLA2. This may reflect the less extensive labelling (approximately 64%) and the higher temperature (40 vs 37 °C) used in our earlier experiments. With PLA2D at a 1:1 dye:protein ratio used here, the lag was somewhat prolonged compared to the native enzyme (30 *vs.* 15 min, respectively, Fig. 2). The observed differences in γ are likely to further result from minor variations in the actual amount of enzyme added. The degree of labelling is difficult to control. In addition, the carboxylic acid succinimidyl esters of Alexa-488 can react with one (or more) of the twelve lysines of the bee venom phospholipase A2. The labelling ratio is determined from spectra, but we have not determined the location of the label. Yet, although the covalent labelling introduces an extra moiety to the protein, the characteristic lag-burst behaviour is retained, thus validating the use of PLA2D for the purposes of this study.

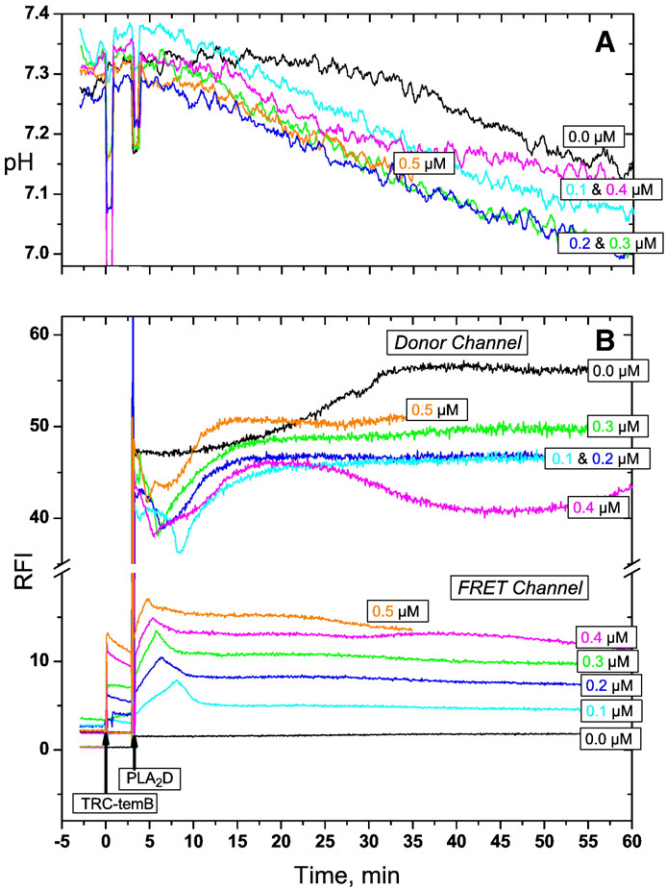

Fig. 1. Time course for FRET between PLA2D and TRC-temB during the hydrolysis of DPPC liposomes monitored as a function of time, with simultaneous measurement of pH to observe the burst. (A) Hydrolysis of the DPPC substrate monitored as a function of time by a decrease in pH. (B) Emission of PLA2D at λ = 520 nm upon excitation at λ_{ex} = 460 nm (donor channel), emission of TRC-temB at λ_{em} = 613 nm upon excitation at λ_{ex} = 460 nm for PLA2D (FRET channel). Medium was water with 1 mM $CaCl_2$ at 37 °C. TRC-temB (0.1–0.5 μM) was first added to the DPPC as indicated, followed after 3 min by the addition of PLA2D (75 nM final concentration). Initial DPPC concentration was 200 μM. The data for 0 μM peptide for panel B and Fig. 5B are from different experiments. The same conditions were used but the experiments were performed on different days. Microheterogeneities of the DPPC liposomes from the different experiment days may change the curves slightly.

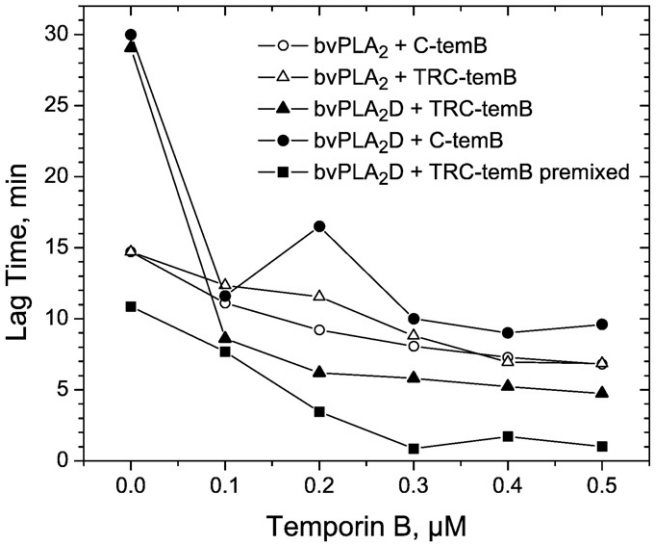

Fig. 2. Lag time γ (in min) in the action of PLA2 on DPPC, shown as a function of peptide concentration. The enzyme-peptide combinations were C-temB and PLA2 (○), TRC-temB and PLA2D (▲, data from Fig. 1), C-temB and PLA2D (●, data from Fig. 5), TRC-temB and PLA2 (△, data from Fig. 4), peptide and enzyme added sequentially, and PLA2D and TRC-temB added simultaneously (pre-mixed) (■, data from Fig. 6).

2.4. FRET

Fluorescence spectra were measured with a spectrofluorometer (Cary) in magnetically stirred 10 mm path length, four window quartz cuvettes thermostated at 37 °C. Unless otherwise indicated all measurements were carried out in a final volume of 1 ml containing 200 μM DPPC or DHPC LUV in 1 mM $CaCl_2$ (unbuffered), with the reactions started by the addition of the indicated amount of temB followed after three min by the addition of PLA2 (final enzyme concentration of 75 nM). Fluorescence of PLA2D (donor) was measured with excitation at 460 nm and emission at 520 nm and that for TRC-temB (acceptor) with excitation at 460 and emission at 613 nm. Bandpasses of 5 nm were used for the excitation and 10 nm for emission. Fluorescence and pH were recorded simultaneously as a function of time using an in-house written script.

2.5. Circular dichroism

CD spectra were measured in a 0.1 mm pathlength quartz cuvette thermostated at 35 °C with a Jasco J-500A spectropolarimeter (Jasco, Tokyo, Japan). The measurements were carried out in a final volume of 200 μl in 1 mM $CaCl_2$ (unbuffered water). Individual spectra were recorded for temB (40 μM), PLA2 (15 μM) and temB with PLA2 added together (40 and 15 μM, respectively). Three averaged scans were recorded from 290 nm to 190 nm, using 1 nm bandwidth, 0.2 nm resolution, 1 s response time, and a scan speed of 20 nm/min.

2.6. Microscopy

Aliquots (200 μl) were taken from the one ml samples of the above indicated experiments into clear glass bottom 96 well plates (Greiner Bio-One, Germany). All experiments were carried out at room temperature (approximately 24 °C). Images were acquired from the microscope fitted with a colour digital camera (DS6031, Canon Europe, Amsterdam, The Netherlands). Confocal fluorescence microscopy was performed using an inverted microscope (IX 70, Olympus, Tokyo, Japan) equipped with a spinning disk confocal scanner (CSU10, Yokogawa, Tokyo, Japan) and a krypton argon ion laser (Melles Griot, Carlsbad, CA). The argon line at 488 nm and a band-pass filter (512–539 nm, green channel) was used for PLA2D visualization, and the

krypton line at 568 nm and a band-pass filter (585–625 nm, red channel) for TRC-temB. Fluorescence images were collected using a Peltier-cooled 12-bit B/W CCD camera (C4742-95, Hamamatsu, Hamamatsu City, Japan) interfaced to a computer and operated by the software (AquaCosmos 1.2) provided by the camera manufacturer. Additional image processing was done using ImageJ software developed at NIH/RSB [39]. Formation of fibres was confirmed by examining eight wells with identical samples containing both liposomes and the enzyme with/without peptide against eight samples containing buffer or buffer and liposomes as controls. These experiments were repeated three times with a consistent number of fibres appearing in the samples. No fibres were observed in the negative controls.

3. Results

TemB as well as several other AMPs have been shown to increase the activity of PLA2 [22]. In order to pursue the mechanisms of this activation in more detail we used TRC-temB, a fluorescent derivative of this peptide, obtained by reacting C-temB, i.e. temB with an additional N-terminal cysteine, with Texas red maleimide. This fluorescent peptide has similar lipid-binding and antimicrobial properties as the native temB [29]. To investigate how the peptide affects the early stages of the interfacial activation we used a saturated phospholipid matrix, L-DPPC, close to its main phase transition temperature, i.e. a system where the lag-burst behaviour is observed [40]. When 0.1 μM TRC-temB was added to the DPPC substrate 3 min before the enzyme addition (Fig. 1A), the lag time decreased from 30 to 9 min (Fig. 2). A further progressive decrease was observed with increasing concentrations from 0.2 to 0.5 μM TRC-temB. Similar decrements in the lag were observed for the native enzyme with TRC-temB (Fig. 4A), PLA2D with C-temB (Fig. 5A) and both enzyme and C-temB lacking the fluorophore (data not shown). Further decrement in the lag time was seen when PLA2D and TRC-temB were mixed prior to their addition to the DPPC liposomes (Fig. 2 and 6). Thus, the presence of temB shortens the latency phase of the phospholipid hydrolysis in a concentration dependent manner.

Possible interactions of PLA2 and temB were studied using FRET between fluorescently labelled enzyme (PLA2D, donor) and peptide (TRC-temB, acceptor). Kinetic measurements were conducted over time with increasing amounts (0.1–0.5 μM) of TRC-temB added 3 min prior to the addition of PLA2D (Fig. 1B). A minor increase in fluorescence was observed in the FRET channel (donor excitation at 460 nm, acceptor emission at 613 nm) when the TRC-temB (acceptor) was added to the liposomes. This increase in fluorescence is due to (residual) direct excitation of the acceptor at the donor excitation wavelength. Following the addition of the donor-labelled enzyme (PLA2D), the fluorescence in the donor channel (donor excitation at 460 nm, and donor emission at 520 nm) decreased gradually during the lag phase reaching a minimum at the burst of enzymatic activity and then returning back to the initial level during the first 5–10 min of hydrolysis. At the same time, reciprocal changes were observed in the FRET channel with the energy transfer between the labelled enzyme and peptide reaching a maximum at the burst point (Fig. 1). Furthermore, in the presence of increasing concentrations of TRC-temB the FRET maximum progressively shifted to earlier times (Fig. 1B), exactly paralleling the shortening of the lag period (Fig. 2) measured from the decrement in pH (Fig. 1A).

FRET was evident in the fluorescence emission measured in the presence of the DPPC substrate liposomes for co-added PLA2D and TRC-temB and comparing these spectra with those for TRC-temB and PLA2D alone (Fig. 3). The spectra were obtained in the latency phase, 2 min after the addition of PLA2D to the liposomes. The excitation wavelength used was 460 nm, which matches the donor (Alexa 488) absorption peak, and also causes a weak direct excitation of Texas Red acceptor. The sample where the donor and acceptor were combined exhibited reduced intensity of PLA2D (donor; emission band around 520 nm) and enhanced intensity of TRC-temB well above the direct excitation level (acceptor; emission band around 610 nm) when

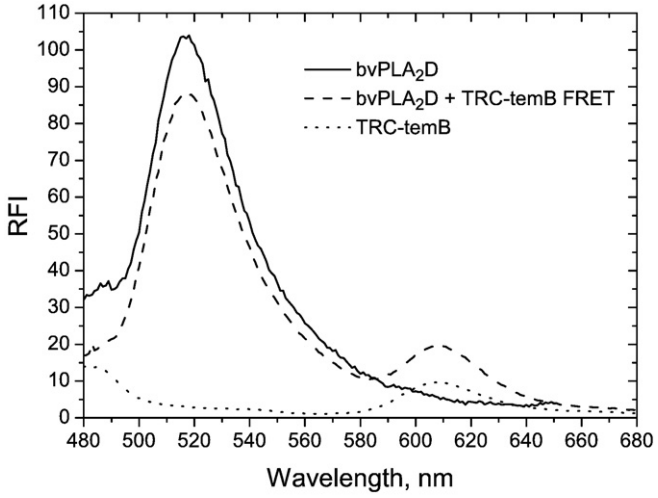

Fig. 3. FRET between PLA2D and TRC-temB interacting with DPPC liposomes. Spectra were recorded for PLA2D alone (*solid line*), PLA2D with TRC-tempB (*dashed line*), and TRC-temB alone (*dotted line*). The excitation wavelength was 460 nm for all spectra. Spectra were recorded 5 min after the addition of PLA2D to DPPC with 0.1 μM of TRC-temB. Other conditions were as described in the legend for Fig. 1.

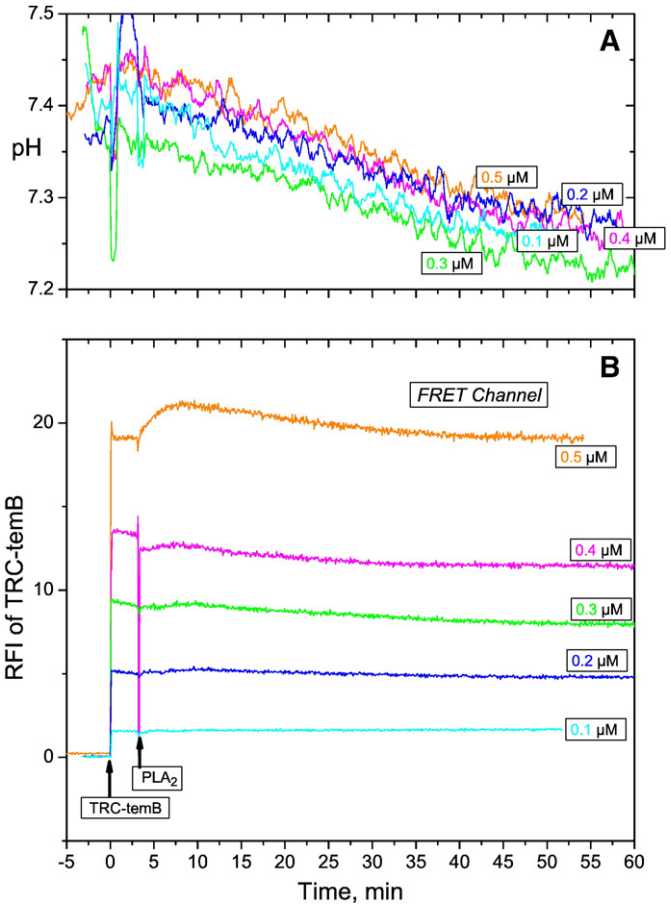

Fig. 4. Time course for FRET between unlabelled PLA2 and increasing concentrations of TRC-temB during hydrolysis of DPPC liposomes, monitored as a function of time. (A) Simultaneous measurement of pH to observe the burst. (B) Emission of TRC-temB at $\lambda_{em} = 613$ nm upon excitation at $\lambda_{ex} = 460$ nm (*FRET channel*). TRC-temB (0.1–0.5 μM) was first added to the DPPC substrate, followed after 3 min by the addition of PLA2 (75 nM final concentration). Conditions were as described in the legend for Fig. 1.

compared to the reference samples. This confirms that in the latency phase of DPPC hydrolysis, energy transfer occurred between the fluorophores attached to PLA2 and temB, thus revealing their close association at this stage. Taken together, the FRET changes suggest progressive association between PLA2 and temB during the latency phase peaking simultaneously with the burst of activity.

In control experiments we used non-labelled PLA2 and TRC-temB (Fig. 4), as well as PLA2D and the non-labelled C-temB (Fig. 5). For PLA2 and TRC-temB a slight increase in the FRET channel is observed (Fig. 4B). This increase in fluorescence may be due to a change in the peptide emission in the DPPC or a direct interaction of TRC-temB with PLA2. However, Texas Red is rather insensitive to microenvironment factors so a change in the peptide conformation may not be observed in this system. In the second set of experiments, using PLA2D and the non-labelled C-temB, the fluorescence of PLA2D decreased slightly at the burst. However, the decrease in donor fluorescence (Fig. 5B all curves) and increase in acceptor fluorescence (Fig. 4B) was less than observed for the enzyme-peptide FRET pair (Fig. 1B). This confirms that the fluorescence changes shown in Fig. 1 arise from FRET, and are not due to the fluorescence changes of the individual fluorophores of the FRET pair. Similar decrements in the lag were observed for the native enzyme with TRC-temB (Fig. 4A), PLA2D with C-temB (Fig. 5A) and both enzyme and C-temB lacking the fluorophores (data not shown). Additionally, TRC-temB and PLA2 were coadded in the presence of liposomes to observe whether the peptide and protein can interact before they associate on the liposome interface (Fig. 6). A decrease in donor fluorescence and an increase in acceptor fluorescence was observed (Fig. 6, panel B) with a less pronounced effect than in Fig. 1. The lag time also decreased for the simultaneous addition (Fig. 6A).

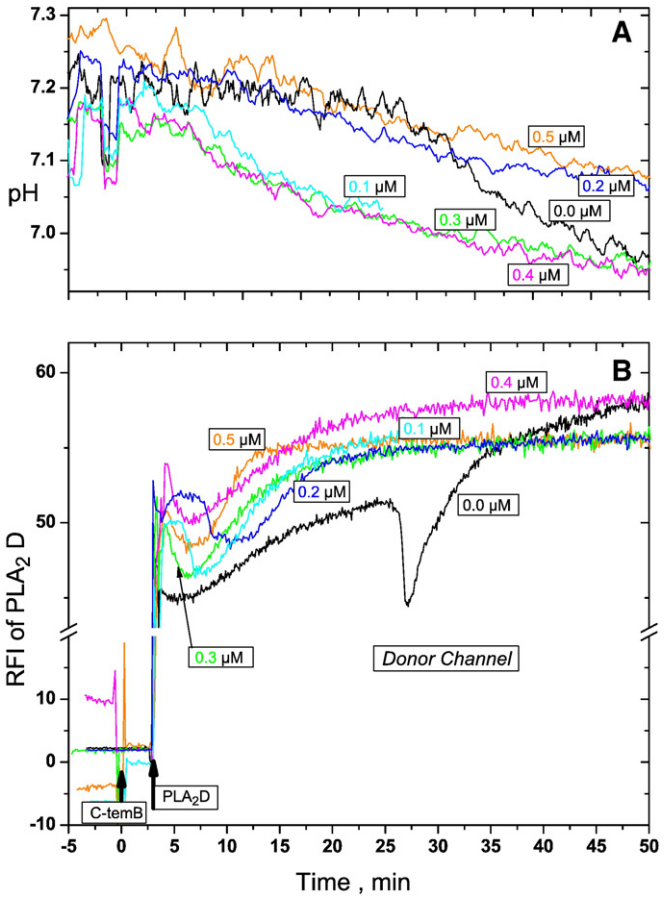

Fig. 5. Lag-burst behavior for FRET by PLA2D in the presence of unlabelled C-temB during hydrolysis of DPPC liposomes. (A) The hydrolysis of the DPPC substrate was monitored as a function of time by decrease in pH. (B) Emission of PLA2D at $\lambda_{em} = 520$ nm upon excitation at $\lambda_{ex} = 460$ nm (*donor channel*). C-temB (0.1–0.5 μM, as indicated) was first added to the DPPC, followed after 3 min by the addition of PLA2D (75 nM final concentration). Conditions were as described in the legend for Fig. 1.

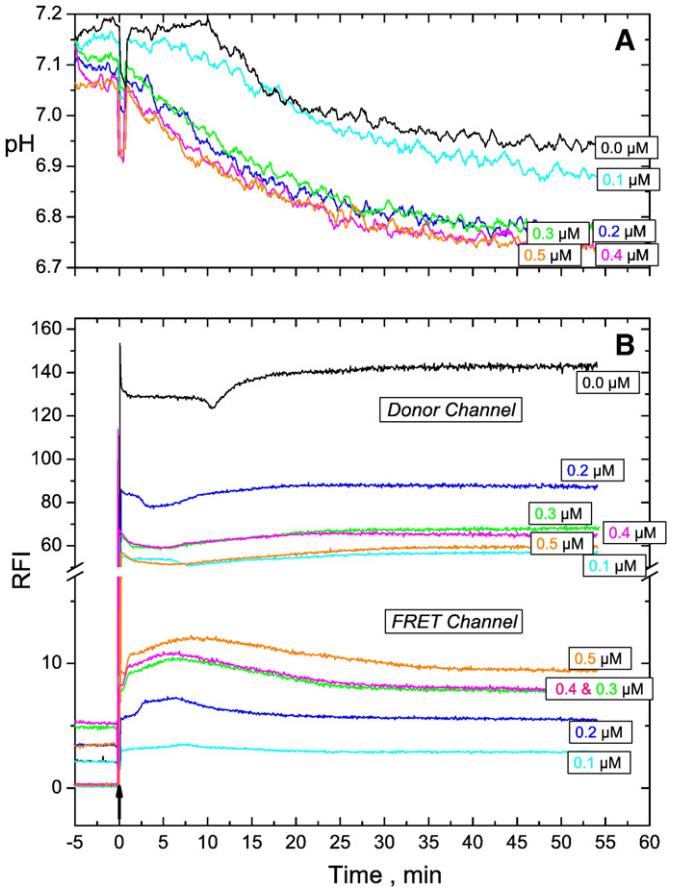

Fig. 6. Time course of FRET between PLA2D and TRC-temB (pre-mixed before addition to DPPC) during hydrolysis of DPPC liposomes, with simultaneous measurement of pH to observe the burst. (A) The hydrolysis of the DPPC substrate monitored as a function of time by decrease in pH. (B) Emission of PLA2D at $\lambda = 520$ nm upon excitation at $\lambda_{ex} = 460$ nm (*donor channel*) and emission of TRC-temB at $\lambda_{em} = 613$ nm upon excitation at $\lambda_{ex} = 460$ nm of PLA2D (*FRET channel*). TRC-temB (0.1–0.5 μM, as indicated) and 75 nM PLA2D were mixed and added to DPPC liposomes (indicated by the arrow). Conditions were as described in the legend for Fig. 1.

As a further control and in order to gain further molecular insight we observed the effect of hydrolysis products on the change in FRET, using the non-hydrolysable enantiomer D-DPPC (Fig. 7A). Differential scanning calorimetry showed identical thermal phase behavior for D-DPPC (data not shown) in our system when compared to L-DPPC [41]. No evidence for aggregation of the liposomes containing products was observed by dynamic light scattering (data not shown). At 0% and with 5 mol% products only a slight increase in FRET and a slight decrease in donor fluorescence were observed. However, with 8, 10 and 15 mol% of both palmitic acid and lysoPC a progressively enhanced FRET was seen with a concomitant decrease in the donor fluorescence (Fig. 7A and B). With an increase in products the FRET enhancement increased with a parallel and opposite change in donor quenching (Fig. 7C). Thus, the reaction products from the PLA2 reaction are needed to induce peptide-PLA2 interaction seen by FRET.

Interactions between PLA2 and temB were investigated also using CD. These spectra (Fig. 8A and B) show that PLA2 and temB interact on the surface of L-DPPC liposomes. PLA2 in the presence of temB increases the absorbance at 208 nm with a significant spectral shift but no change is detected at 190 nm. Subtracting the spectra for temB as such from the spectra measured for the coadded peptide and enzyme does not abolish this change (Fig. 8A). Furthermore, the temB spectrum changes in the presence of PLA2 showing a larger

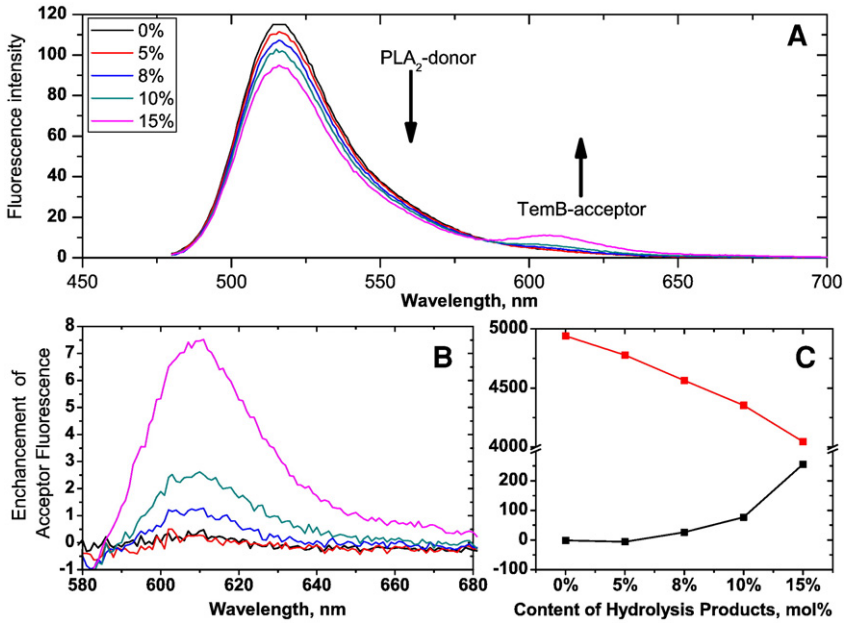

Fig. 7. (A) FRET between PLA2D and TRC-temB interacting with D-DPPC liposomes and increasing amount of hydrolysis products lysoPC:Palmitic Acid (1:1 molar ratio) as indicated. Full spectra were recorded for PLA2D with TRC-temB. (B) Corrected spectra for TRC-temB acceptor enhancement. (C) Donor quenching and acceptor enhancement as a function of increasing amount the products. The excitation wavelength was 460 nm. Spectra were recorded 3 min after the addition of PLA2D to D-DPPC with (products at 0, 5, 8, 10, 15 mol%) and 0.1 μM of TRC-temB. Other conditions were as described in the legend for Fig. 1.

absorbance when the contribution from PLA2 is subtracted (Fig. 8B). A change in temB from a random coil to a more α-helical conformation occurs at different peptide lipid ratios (see Appendix, S3).

Both temB and PLA2 form, in the presence of negatively charged lipids, amyloid-type fibres [13,29] and for PLA2 we have suggested that this process causes a conformational change into a transient high activity state [13]. Along these lines, we hypothesized that the formation of heterooligomers by PLA2 and temB would be responsible for the activation by temB of PLA2, promoting enzyme aggregation into an active conformation. Subsequently, this would be followed by the formation of 'mature' amyloid fibers, with the enzyme switching into an inactive state. Supporting this mechanism, examination of the reaction mixture (approxim. 1 h after the enzyme addition) under a bright field microscope revealed macroscopic fibres (>100 μm in length, Fig. 9A). Interestingly, these fibrils were fluorescent in both the green (PLA2D) and red (TRC-temB) channels (Fig. 9B and C, respectively). The intensity observed in the red channel (Fig. 9C) is higher than in the green channel (Fig. 9C). These data can be rationalized by *i*) the higher TRC-temB concentration compared to PLA2D, and *ii*) FRET from the PLA2D to the TRC-temB. In addition, there is a poorly understood loss of fluorescence due to the formation of amyloid-like fibres [42].

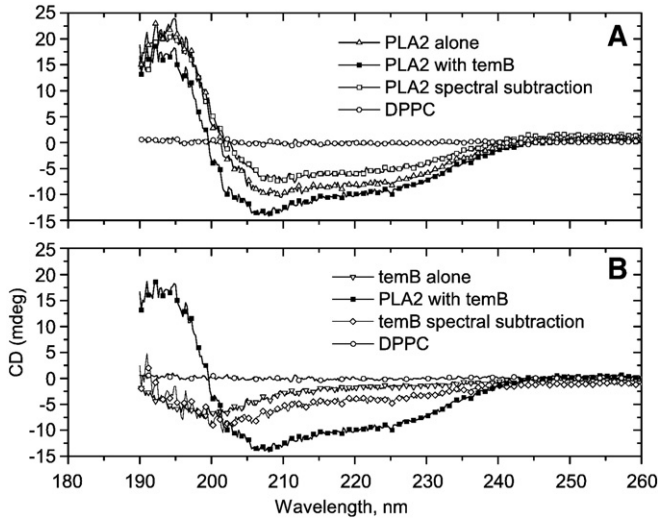

Fig. 8. Circular Dichroism PLA2 and temB with DPPC liposomes. Measurements were carried out in a final volume of 200 μl in 1 mM $CaCl_2$ (unbuffered water) with DPPC LUV. Individual spectra were recorded for DPPC LUV (200 μM, ○), PLA2 with temB (15 μM and 40 μM, ■). (A) PLA2 alone (15 μM, △), PLA2 spectral subtraction (□). (B) temB alone (40 μM, ▽), temB spectral subtraction (◊). Three averaged scans of CD were measured. Spectra were recorded 35 °C from 290 nm to 190 nm, using 1 nm bandwidth, 0.2 nm resolution, 1 s response time, and a scan speed of 20 nm/min.

4. Discussion

To summarize, C-temB, and TRC-temB decrease the latency phase of PLA2 when added to DPPC liposomes (Figs. 1, 3–6). The activation of PLA2 through reduction of the lag phase in phospholipid hydrolysis could be explained by at least two distinct mechanisms. First, the activation could be mediated by a perturbation of the lipid bilayer structure caused by peptide binding. Indeed, temB binding and insertion cause extensive short-range (i.e. enhanced lipid acyl chain order and segregation of negatively charged lipids, [28,31] as well as long-range perturbation of the bilayer structure [43]. Second, temB can directly bind PLA2 and form supramolecular structures, thus activating the enzyme directly by altering its conformation.

Subsequent to the burst, following the onset of maximal hydrolysis the vesicles disrupt and the lipid organization changes dramatically with complex and poorly understood polymorphism [44-46]. Optically, this is evident as a pronounced increase in light scattering after the burst, as demonstrated in several studies (e.g. [10], Fig. 1 in reference [13]). While detailed understanding of the molecular arrangements during the reaction would obviously be interesting, taking into account the massive transformation in the 3-D organization, we are not aware of a technique, which would make it possible to keep track of intervesicular contacts and the origin of the different components in the aggregate. Importantly, in the current study we were interested in the process resulting in the activation of PLA2,

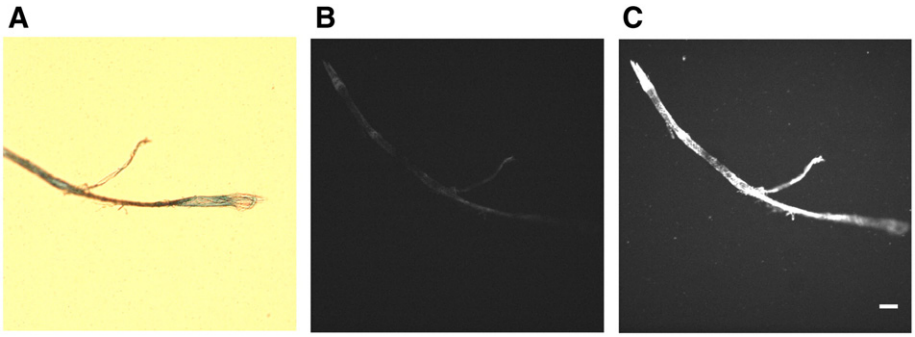

Fig. 9. Fibrils formed after reacting DPPC with PLA2D and TRC-temB as described for Fig. 1. Aliquots (200 μl) of the reaction mixture taken 1 h after starting the reaction were transferred from cuvettes into a 96 well plate for fluorescence microscopy. (A) shows a bright field DIC image of a fibril. Fluorescence image of 0.4 μM TRC-temB with 75 nM PLA2D cofibrils using $\lambda_{ex} = 488$ nm and $\lambda_{em} = 512–539$ nm filters (green fluorescence, (B), and $\lambda_{ex} = 568$ nm and $\lambda_{em} = 585–625$ nm filters (red fluorescence, (C) of the same fibril. The scale bar corresponds to 20 μm.

focusing on the molecular scale events preceding the burst. Both literature data and our observations show that the light scattering during the lag is very close to the scattering level of individual liposomes, revealing that there is no significant liposome aggregation or morphological transformations preceding the burst.

Increasing the concentration of TRC-temB from 0.1 μM to 0.5 μM progressively decreased the lag. The shortest lag was observed when PLA2 and the peptide were mixed before their addition to the phospholipid substrate. However, using anisotropy and FRET we did not find any evidence for an interaction in solution with just the protein and peptide present (in the absence of liposomes, data not shown). It is possible that in solution at low ionic strength electrostatic repulsion repel the peptide and protein from each other, as they both have a net positive charge at neutral pH. It is possible, that the complex formation resulting in PLA2 activation would be most efficient, when PLA2 and temB are in the conformations prevailing immediately following their surface association. To this end, both PLA2 and temB are known to undergo conformational changes upon transfer from solution to the lipid interface, further connected to aggregation and formation of amyloid-type fibers [13,29,47]. Association with the negatively charged reaction product (FFA) overcomes the electrostatic repulsion between the peptide and enzyme on the surface of substrate bilayer, allowing interaction to occur, as demonstrated by our FRET experiments with bee venom PLA2 and temB. Our CD data demonstrate interaction of PLA2 and temB on the surface of DPPC (Fig. 8A and B) and a change in temB from a random coil to a more α-helical conformation at different peptide lipid ratios (see Appendix, S3).

Changes in enzyme conformation at the burst have been demonstrated, as observed by us using Alexa-488 and Alexa-568 labelled PLA2 [13], while Bell et al. [10] reported an increase in the intrinsic Trp fluorescence of PLA2. Here we show an increase in acceptor fluorescence (FRET) when the donor is added (Fig. 3). The FRET data was corrected to take into account this increase in donor fluorescence in the spectra. We observed the full spectra containing both donor and acceptor over a number of time points and found that the increase in donor fluorescence was independent of a FRET increase. Homotransfer or homoFRET may take place for identical fluorophores such as BODIPY that display a small Stokes shift [48]. For the probe used with bvPLA2D, Alexa-488, the Stokes shift is larger and homoFRET is small. In addition homoFRET will not lead to a change in fluorescence emission or a change in the lifetime because excitation energy is transferred to the same probe. HomoFRET does increase the depolarization when there is an increase in the concentration of probes in a viscous solution. As homoFRET should not affect the emission intensity, it is unlikely that this process would be involved in the system studied here.

FRET was observed between the TRC-temB and the PLA2D (Fig. 1) when reacting with the DPPC substrate, indicating a direct TRC-tempB and PLA2D interaction on the surface. With increasing concentrations of TRC-temB there was a progressive increase in FRET, with a maximum at the burst in the enzyme activity for PLA2D. PLA2 produces lysoPC and negatively charged FFA prior to the burst point and a critical content of these products is required to initiate the burst [20]. TemB has been shown to segregate anionic lipids in a binary membrane [28]. The lag-burst behavior and the changes in chemical composition (accumulation of the reaction products) have been very thoroughly characterized in previous studies [10,49,50]. In brief, these results show very slow, time dependent accumulation of the products until at the burst approx. 8 mol% of both fatty acid and lysoPC (1:1 stoichiometry) have been formed. At this point, the enzyme activity increases very rapidly, resulting in a significant large scale reorganization of the remaining substrate and the reaction products, readily visible as pronounced aggregation and turbidity. Accordingly, we only needed to observe the burst point, which is most easily detected by the rate of decrease in pH, as described in several earlier studies [10,38]. For an efficient FRET a hydrolysable interface is needed viz. L-DPPC and Ca^{2+} need to be present. Further, the catalytic activity is needed for peptide-protein association and in the presence of EDTA FRET is not observed. This is evident with both DPPC and POPC as a substrate (data not shown). After the enzyme addition several minutes are needed before FRET increases, with a parallel decrease in donor fluorescence. It is apparent that this local accumulation of hydrolytic products is needed for oligomerization of the PLA2 at the interface. Furthermore, this local accumulation of the hydrolytic products FFA and lysoPC during the lag appears to be needed also for TRC-temB-PLA2D association, as a substantial and an increasing intensity of FRET is seen with increasing amounts of products present in D-DPPC liposomes. The reaction products viz. lysoPC and FFA added into a non-hydrolysable substrate enantiomer D-DPPC increase FRET between the PLA2D and TRC-temB (Fig. 7). Vesicle size measurements of D-DPPC liposomes with different concentrations of products by dynamic light scattering measurements revealed no evidence for vesicle aggregation. Therefore, FRET is a consequence of the temB-PLA2 association on the surface of individual liposomes (Fig. 7).

Cholesterol attenuates the association of temB with phospholipid bilayers [29] and Bell et al. showed [51] that a high content of cholesterol protects cells from hydrolytic enzymes such as PLA2. They also showed that the behavior of PLA2 in this respect is comparable in biological membranes and in model membranes. Similar biophysical studies by Simonsen show that cholesterol is a key lipid in regulating PLA2 activation and suggests that cholesterol is able to partially or completely block the activation of PLA2 on ternary model membranes [52]. While the effects of cholesterol are of interest, experiments described here aimed to the clarification of the mechanism of activation of PLA2 by temB. The effects of cholesterol are likely to be complex and warrant an extensive study of its own.

Along these lines, melittin, a 26 residue peptide present in bee venom, has been shown to both activate and inhibit PLA2 depending on its concentration [25,26,53] and this activation correlates with the formation of a complex that involves PLA2, melittin, phospholipid substrate, and Ca^{+2} [25]. Similarly to temB melittin is capable of penetrating and solubilizing membranes [54], and possesses antimicrobial activity. We have recently suggested the interfacial activation of PLA2 to be caused by the emergence of highly active enzyme oligomers, existing as intermediates in the aggregation-refolding path yielding at the end inactive amyloid-type fibres [13]. In line with the above, we hypothesized that the formation of heterooligomers by PLA2 and temB would underlie the activation of this enzyme by the latter AMP, which also forms itself, in the presence of negatively charged lipids, amyloid-type fibres [29]. In the light of the present results this would be feasible. First, our data show specific lipid structures (FFA and lysoPC) to be required for close association of temB and PLA2, seen by FRET (present study and Code et al., to be published). Second, under conditions where activation is seen, also amyloid-type fibrils are seen, whereas in the absence of the reaction products these fibres do not form. In the zwitterionic DPPC liposomes temB as such does not form fibrils. Third, the fibres incorporate both TRC-temB and PLA2D, as seen by their fluorescence. The amount of lipids and placement of lipids in the amyloid-like structure is not clearly understood however. The other membrane partitioning and amyloid formation prone, PLA2 activating AMPs mentioned above may form similar supramolecular complexes.

Amyloid formation seems to be required also for the activation of PLA2 by the Alzheimer Aβ fragments. Accordingly, peptide fragments $A\beta_{1-42}$ and $A\beta_{25-35}$ activate PLA2 whereas $A\beta_{1-25}$ has no effect [8].

Our data show that temB promotes amyloid cofibril formation with PLA2 in the lipid membrane. TemB may serve as "molecular glue" fitting in between the PLA2 monomers and oligomers and thus promoting PLA2 oligomerization, via the formation of catalytically active heterooligomers. Heterooligomers have been observed between α-synuclein upon seeding with bovine insulin, lysozyme, and insulin fibrils [55]. Glyceraldehyde-3-phosphate dehydrogenase has been found to coaggregate with α-synuclein [56]. It has been speculated that IAPP may induce nucleation of oligomer formation, thus promoting neuronal disorders [57,58]. In this context it is of interest that also apolipoprotein C-II (apoC-II), a peptide activator of another lipolytic enzyme, lipoprotein lipase (LPL), forms amyloid, and this amyloid formation is enhanced by lipids [59]. Furthermore, the lipoprotein lipase activating domain of apoC-II coincides with the amyloid forming residues of this apolipoprotein [60]. In this regard, while several possibilities have been proposed [61,62], the mechanism of activation of lipoprotein lipase by apoC-II has remained elusive. Our current results tempt speculation along analogous lines to the activation of PLA2 by temB described here, viz. the formation apoC-II/LPL amyloid-type heterooligomers.

Acknowledgments

The authors wish to thank Dr. Juha-Matti Alakoskela and Lucie Khemtémourian for helpful discussions and help with data collection scripts, Prof. Ben de Kruijff for suggesting the use of D-DPPC, and Kristiina Söderholm for technical assistance. HBBG is supported by grants from the Marie Curie EST Training Network (C.C.) and Incoming International Fellowship (Y.D.), the Academy of Finland, and Sigrid Jusélius Foundation.

Appendix A. Supplementary data

Supplementary data associated with this article can be found, in the online version, at doi:10.1016/j.bbamem.2009.03.002.

References

[1] D.A. Six, E.A. Dennis, The expanding superfamily of phospholipase A(2) enzymes: classification and characterization, Biochim. Biophys. Acta (2000) (1488) 1–19.
[2] D.L. Scott, S.P. White, Z. Otwinowski, W. Yuan, M.H. Gelb, P.B. Sigler, Interfacial catalysis: the mechanism of phospholipase A2, Science 250 (1990) 1541–1546.
[3] W.A. Pieterson, J.C. Vidal, J.J. Volwerk, G.H. de Haas, Zymogen-catalyzed hydrolysis of monomeric substrates and the presence of a recognition site for lipid–water interfaces in phospholipase A2, Biochemistry 13 (1974) 1455–1460.
[4] R. Verger, M.C. Mieras, G.H. de Haas, Action of phospholipase Aat interfaces, J.Biol. Chem. 248 (1973) 4023–4034.
[5] M.A. Wells, The mechanism of interfacial activation of phospholipase A2, Biochemistry 13 (1974) 2248–2257.
[6] J.A. Op den Kamp, M.T. Kauerz, L.L. van Deenen, Action of pancreatic phospholipase A2 on phosphatidylcholine bilayers in different physical states, Biochim. Biophys. Acta 406 (1975) 169–177.
[7] R. Apitz-Castro, M.K. Jain, G.H. De Haas, Origin of the latency phase during the action of phospholipase A2 on unmodified phosphatidylcholine vesicles, Biochim. Biophys. Acta 688 (1982) 349–356.
[8] J.Y. Lehtonen, J.M. Holopainen, P.K.J. Kinnunen, Activation of phospholipase A2 by amyloid beta-peptides in vitro, Biochemistry 35 (1996) 9407–9414.
[9] A. Halperin, O.G. Mouritsen, Role of lipid protrusions in the function of interfacial enzymes, Eur. Biophys. J 34 (2005) 967–971.
[10] J.D. Bell, R.L. Biltonen, The temporal sequence of events in the activation of phospholipase A2 by lipid vesicles. Studies with the monomeric enzyme from *Agkistrodon piscivorus piscivorus*, J. Biol. Chem. 264 (1989) 12194–12200.
[11] C. Leidy, O.G. Mouritsen, K. Jorgensen, G.H. Peters, Evolution of a rippled membrane during phospholipase A2 hydrolysis studied by time-resolved AFM, Biophys. J. 87 (2004) 408–418.
[12] T. Thuren, A.P. Tulkki, J.A. Virtanen, P.K.J. Kinnunen, Triggering of the activity of phospholipase A2 by an electric field, Biochemistry 26 (1987) 4907–4910.
[13] C. Code, Y. Domanov, A. Jutila, P.K.J. Kinnunen, Amyloid-type fiber formation in control of enzyme action: interfacial activation of phospholipase A2, Biophys. J. 95 (2008) 215–224.
[14] S.A. Tatulian, R.L. Biltonen, L.K. Tamm, Structural changes in a secretory phospholipase A2 induced by membrane binding: a clue to interfacial activation? J. Mol. Biol. 268 (1997) 809–815.
[15] S.A. Tatulian, Toward understanding interfacial activation of secretory phospholipase A2 (PLA2): membrane surface properties and membrane-induced structural changes in the enzyme contribute synergistically to PLA2 activation, Biophys. J. 80 (2001) 789–800.
[16] J.D. Hille, M.R. Egmond, R. Dijkman, M.G. van Oort, B. Jirgensons, G.H. de Haas, Aggregation of porcine pancreatic phospholipase A2 and its zymogen induced by submicellar concentrations of negatively charged detergents, Biochemistry 22 (1983) 5347–5353.
[17] T.L. Hazlett, R.A. Deems, E.A. Dennis, Activation, aggregation, inhibition and the mechanism of phospholipase A2, Adv. Exp. Med. Biol 279 (1990) 49–64.
[18] D.W. Grainger, A. Reichert, H. Ringsdorf, C. Salesse, Hydrolytic action of phospholipase A2 in monolayers in the phase transition region: direct observation of enzyme domain formation using fluorescence microscopy, Biochim. Biophys. Acta 1023 (1990) 365–379.
[19] K.M. Maloney, M. Grandbois, C. Salesse, D.W. Grainger, A. Reichert, Membrane microstructural templates for enzyme domain formation, J. Mol. Recognit. 9 (1996) 368–374.
[20] W.R. Burack, M.E. Gadd, R.L. Biltonen, Modulation of phospholipase A2: identification of an inactive membrane-bound state, Biochemistry 34 (1995) 14819–14828.
[21] E. Chibowski, L. Holysz, M. Jurak, Effect of lipolytic enzyme on wettability and topography of phospholipid layers deposited on solid support, Colloids Surf., A Physiocochem. Eng. Aspects 321 (2008) 131–136.
[22] H. Zhao, P.K.J Kinnunen, Modulation of the activity of secretory phospholipase A2 by antimicrobial peptides, Antimicrob. Agents Chemother. 47 (2003) 965–971.
[23] S. Pochet, S. Tandel, S. Querriere, M. Tre-Hardy, M. Garcia-Marcos, M. De Lorenzi, M. Vandenbranden, A. Marino, M. Devleeschouwer, J.P. Dehaye, Modulation by LL-37 of the responses of salivary glands to purinergic agonists, Mol. Pharmacol. 69 (2006) 2037–2046.
[24] G. Signor, S. Mammi, E. Peggion, H. Ringsdorf, A. Wagenknecht, Interaction of bombolitin III with phospholipid monolayers and liposomes and effect on the activity of phospholipase A2, Biochemistry 33 (1994) 6659–6670.
[25] I. Mingarro, E. Perez-Paya, C. Pinilla, J.R. Appel, R.A. Houghten, S.E. Blondelle, Activation of bee venom phospholipase A2 through a peptide–enzyme complex, FEBS Lett. 372 (1995) 131–134.
[26] K. Koumanov, A. Momchilova, C. Wolf, Bimodal regulatory effect of melittin and phospholipase A2-activating protein on human type II secretory phospholipase A2, Cell Biol. Int. 27 (2003) 871–877.
[27] H. Zhao, J.P. Mattila, J.M. Holopainen, P.K.J. Kinnunen, Comparison of the membrane association of two antimicrobial peptides, magainin 2 and indolicidin, Biophys. J. 81 (2001) 2979–2991.
[28] H. Zhao, A.C. Rinaldi, A. Di Giulio, M. Simmaco, P.K.J. Kinnunen, Interactions of the antimicrobial peptides temporins with model biomembranes. Comparison of temporins B and L, Biochemistry 41 (2002) 4425–4436.
[29] R. Sood, Y. Domanov, P.K.J. Kinnunen, Fluorescent temporinB , derivative and its binding to liposomes, J. Fluoresc. 17 (2007) 223–234.

[30] M. Simmaco, G. Mignogna, D. Barra, F. Bossa, Antimicrobial peptides from skin secretions of *Rana esculenta*. Molecular cloning of cDNAs encoding esculentin and brevinins and isolation of new active peptides, J. Biol. Chem. 269 (1994) 11956–11961.
[31] A.C. Rinaldi, M.L. Mangoni, A. Rufo, C. Luzi, D. Barra, H. Zhao, P.K. Kinnunen, A. Bozzi, A. Di Giulio, M. Simmaco, L. Temporin, Antimicrobial, haemolytic and cytotoxic activities, and effects on membrane permeabilization in lipid vesicles, Biochem. J. 368 (2002) 91–100.
[32] S. Carotenuto, M.R. Malfi, P. Saviello, I. Campiglia, M.L. Gomez-Monterrey, L.M. Mangoni, E. Gaddi, P. Novellino, A. Grieco, Different molecular mechanism underlying antimicrobial and hemolytic actions of temporins A and L, J. Med. Chem. 51 (2008) 2354–2362.
[33] H. Zhao, R. Sood, A. Jutila, S. Bose, G. Fimland, J. Nissen-Meyer, P.K.J. Kinnunen, Interaction of the antimicrobial peptide pheromone Plantaricin A with model membranes: Implications for a novel mechanism of action, Biochim. Biophys. Acta 1758 (2006) 1461–1474.
[34] R. Sood, Y. Domanov, M. Pietiainen, V.P. Kontinen, P.K.J Kinnunen, Binding of LL-37 to model biomembranes: insight into target vs host cell recognition, Biochim. Biophys. Acta 1778 (2008) 983–996.
[35] H. Zhao, E.K. Tuominen, P.K.J. Kinnunen, Formation of amyloid fibers triggered by phosphatidylserine-containing membranes, Biochemistry 43 (2004) 10302–10307.
[36] H. Zhao, A. Jutila, T. Nurminen, S.A. Wickstrom, J. Keski-Oja, P.K.J. Kinnunen, Binding of endostatin to phosphatidylserine-containing membranes and formation of amyloid-like fibers, Biochemistry 44 (2005) 2857–2863.
[37] F. Ghomashchi, Y. Lin, M.S. Hixon, B.Z. Yu, R. Annand, M.K. Jain, M.H. Gelb, Interfacial recognition by bee venom phospholipase A2: insights into nonelectrostatic molecular determinants by charge reversal mutagenesis, Biochemistry 37 (1998) 6697–6710.
[38] T. Honger, K. Jorgensen, R.L. Biltonen, O.G. Mouritsen, Systematic relationship between phospholipase A2 activity and dynamic lipid bilayer microheterogeneity, Biochemistry 35 (1996) 9003–9006.
[39] W. Rasband, Image J. Public domain java image processing program. Http://rsbweb.Nih.gov/ij (2005).
[40] O.G. Mouritsen, Life as a Matter of Fat The Emerging Science of Lipidomics. Springer-Verlag, Berlin Heidelberg New York Series: The Frontiers Collection, 2005, pp. 148-150.
[41] W.R. Burack, Q. Yuan, R.L. Biltonen, Role of lateral phase separation in the modulation of phospholipase A2 activity, Biochemistry 32 (1993) 583–589.
[42] A. Dusa, J. Kaylor, S. Edridge, N. Bodner, D.P. Hong, A.L. Fink, Characterization of oligomers during alpha-synuclein aggregation using intrinsic tryptophan fluorescence, Biochemistry 45 (2006) 2752–2760.
[43] Y.A. Domanov, P.K.J Kinnunen, Antimicrobial peptides temporins B and L induce formation of tubular lipid protrusions from supported phospholipid bilayers, Biophys. J. 91 (2006) 4427–4439.
[44] S.A. Sanchez, L.A. Bagatolli, E. Gratton, T.L. Hazlett, A two-photon view of an enzyme at work, *Crotalus atrox* venom PLA2 interaction with single-lipid and mixed-lipid giant unilamellar vesicles, Biophys. J. 82 (2002) 2232–2243.
[45] T. Honger, Interplay Between Dynamic Properties and Functionality of Biomembranes, Dynamic Microstructure, Membrane Flexibility, and Morphological Instability Induced by Phospholipase A2. Doctoral Thesis, Department of Physical Chemistry, The Technical University of Denmark (1994) 1–101.
[46] P. Hoyrup, Phospholipase A2 activity in relation to the physical properties of lipid bilayers. Doctoral Thesis, Department of Chemistry, The Technical University of Denmark (2001) 1–130.
[47] T. Ahmed, S.M. Kelly, A.J. Lawrence, M. Mezna, N.C. Price, Conformational changes associated with activation of bee venom phospholipase A2, J. Biochem. 120 (1996) 1224–1231.
[48] Y. Yan, G. Marriott, Analysis of protein interactions using fluorescence technologies, Curr. Opin. Chem. Biol. 7 (2003) 635–640.
[49] W.R. Burack, Q. Yuan, R.L. Biltonen, Role of lateral phase separation in the modulation of phospholipase A2 activity, Biochemistry 32 (1993) 583–589.
[50] P. Hoyrup, O.G. Mouritsen, K. Jorgensen, Phospholipase A(2) activity towards vesicles of DPPC and DMPC-DSPC containing small amounts of SMPC, Biochim. Biophys. Acta 1515 (2001) 133–143.
[51] A.L. Heiner, E. Gibbons, J.L. Fairbourn, L.J. Gonzalez, C.O. McLemore, T.J. Brueseke, A.M. Judd, J.D. Bell, Effects of cholesterol on physical properties of human erythrocyte membranes: impact on susceptibility to hydrolysis by secretory phospholipase A2, Biophys. J. 94 (2008) 3084–3093.
[52] A.C. Simonsen, Activation of phospholipase A2 by ternary model membranes, Biophys. J. 94 (2008) 3966–3975.
[53] S.S. Saini, J.W. Peterson, A.K. Chopra, Melittin binds to secretory phospholipase A2 and inhibits its enzymatic activity, Biochem. Biophys. Res. Commun 238 (1997) 436–442.
[54] L. Yang, T.A. Harroun, T.M. Weiss, L. Ding, H.W. Huang, Barrel-stave model or toroidal model? A case study on melittin pores, Biophys. J. 81 (2001) 1475–1485.
[55] H. Yagi, E. Kusaka, K. Hongo, T. Mizobata, Y. Kawata, Amyloid fibril formation of alpha-synuclein is accelerated by preformed amyloid seeds of other proteins: implications for the mechanism of transmissible conformational diseases, J. Biol. Chem. 280 (2005) 38609–38616.
[56] K. Tsuchiya, H. Tajima, T. Kuwae, T. Takeshima, T. Nakano, M. Tanaka, K. Sunaga, Y. Fukuhara, K. Nakashima, E. Ohama, H. Mochizuki, Y. Mizuno, N. Katsube, R. Ishitani, Pro-apoptotic protein glyceraldehyde-3-phosphate dehydrogenase promotes the formation of Lewy body-like inclusions, Eur. J. Neurosci. 21 (2005) 317–326.
[57] L.M. Yan, A. Velkova, M. Tatarek-Nossol, E. Andreetto, A. Kapurniotu, IAPP mimic blocks Abeta cytotoxic self-assembly: cross-suppression of amyloid toxicity of Abeta and IAPP suggests a molecular link between Alzheimer's disease and type II diabetes, Angew Chem. Int. Ed. Engl. 46 (2007) 1246–1252.
[58] B. O'Nuallain, A.D. Williams, P. Westermark, R. Wetzel, Seeding specificity in amyloid growth induced by heterologous fibrils, J. Biol. Chem. 279 (2004) 17490–17499.
[59] L.M. Wilson, Y.F. Mok, K.J. Binger, M.D. Griffin, H.D. Mertens, F. Lin, J.D. Wade, P.R. Gooley, G.J. Howlett, A structural core within apolipoprotein C-II amyloid fibrils identified using hydrogen exchange and proteolysis, J. Mol. Biol. 366 (2007) 1639–1651.
[60] P.K.J Kinnunen, R.L. Jackson, L.C. Smith, A.M. Gotto Jr., J.T. Sparrow, Activation of lipoprotein lipase by native and synthetic fragments of human plasma apolipoprotein C-II, Proc. Natl. Acad. Sci. U. S. A. 74 (1977) 4848–4851.
[61] P.K.J. Kinnunen, J.A. Virtanen, P. Vainio, in: A.M. Gotto Jr, R. Paoletti (Eds.), Lipoprotein lipase and hepatic endothelial lipase: Their roles in plasma lipoprotein metabolism, Raven Press, New York, 1983.
[62] L.C. Smith, H.J. Pownall, Lipoprotein lipase, in: B. Borgström, H.L. Brockman (Eds.), Lipases, Elsevier, Amsterdam, 1984.